Diabetes, Metabolic Syndrome and Obesity

Dovepress

open access to scientific and medical research

Open Access Full Text Article

ORIGINAL RESEARCH

# Effect of Semaglutide and Empagliflozin on Pulmonary Structure and Proteomics in Obese Mice

Yu Yang[1,2], Xiaoyu Pan[1,3], Shuchun Chen[1,3]

[1]Department of Internal Medicine, Hebei Medical University, Shijiazhuang, People's Republic of China; [2]Department of Pharmacy, The Second Hospital of Hebei Medical University, Shijiazhuang, People's Republic of China; [3]Department of Endocrinology, Hebei General Hospital, Shijiazhuang, People's Republic of China

Correspondence: Shuchun Chen, Department of Endocrinology, Hebei General Hospital, 348 Heping West Road, Shijiazhuang, Hebei, 050051, People's Republic of China, Tel/Fax +86 311 85988406, Email chenshuchunwork88@163.com

**Objective:** This study utilized proteomics to investigate changes in protein expression associated with lung health in obese mice exposed to semaglutide and empagliflozin through a high-fat diet.

**Methods:** Twenty-eight male C57BL/6JC mice were randomly assigned to two groups: a control diet group (n = 7) and a high-fat diet group (n = 21). The HFD group was further divided into three groups: HFD group (n = 7), Sema group (n = 7), and Empa group (n = 7). Post-treatment, mice underwent assessments including glucose tolerance, lipids, oxidative stress markers, body weight, lung weight, and structure. Proteomics identified differentially expressed proteins (DEPs) in lung tissue, and bioinformatics analyzed the biological processes and functions of these proteins.

**Results:** Semaglutide and empagliflozin significantly attenuated obesity-induced hyperglycemia, abnormal lipid metabolism, oxidative stress response, and can decrease alveolar wall thickness, enlarge alveolar lumen, and reduce collagen content in lung tissue. Both medications also attenuated lung elastic fibre cracking and disintegration. In the HFD/NCD group, there were 66 DEPs, comprising 30 proteins that were increased and 36 that were decreased. Twenty-three DEPs overlapped between Sema/HFD and Empa/HFD, with 11 up-regulated and 12 down-regulated simultaneously. After analysing DEPs in different groups, four proteins - LYVE1, BRAF, RGCC, and CHMP5 - were all downregulated in the HFD group and upregulated by semaglutide and empagliflozin treatment.

**Conclusion:** This study demonstrates that obesity induced by a high-fat diet causes a reduction in the expression of LYVE1, BRAF, RGCC, and CHMP5 proteins, potentially affecting lung function and structure in mice. Significantly, the administration of semaglutide and empagliflozin elevates the levels of these proteins, potentially offering therapeutic benefits against lung injury caused by obesity. Merging semaglutide with empagliflozin may exert a more pronounced impact.

**Keywords:** semaglutide, empagliflozin, proteomics, obesity, pulmonary structure

## Introduction

In recent years, there has been a sharp rise in the prevalence of obesity around the globe. The World Health Organization's most recent figures indicate that the amount of adults worldwide who are overweight or obese is close to 2 billion, and this figure is on the rise.[1] Obesity, characterized by an excessive accumulation of fat in fat cells, is a complex and chronic condition associated with resistance to insulin, elevated blood pressure, and irregular lipid concentrations.[2] Obesity has a direct impact on the mechanical properties of the lung and chest wall by causing fat to accumulate in the mediastinum and abdominal and thoracic cavities.[3] Consequently, the diaphragm is elevated, restricting its downward movement and resulting in heightened pleural pressure and reduced functional residual capacity.[4,5] Obesity can lead to a decrease in lung, chest wall, and respiratory system compliance, potentially contributing to respiratory issues commonly experienced by many obese individuals.[6] The multifactorial influence of obesity on the lung involves mechanical injury and the role of various inflammatory mediators produced by excess adipose tissue and infiltrating immune cells. Obesity-related lung disease exhibits distinct characteristics, affecting both disease severity and treatment effectiveness, compared to other pulmonary

Received: 22 December 2023
Accepted: 28 February 2024
Published: 11 March 2024

pathologies. Notably, obstructive sleep apnea and obesity hypoventilation syndrome are closely associated with obesity.[7,8] Obesity has also been linked to a variety of other respiratory illnesses, such as asthma, COPD, and pulmonary fibrosis.[9–11]

In contrast to genomics, proteomics aims to elucidate the entirety of proteins expressed within a cell or organism.[12] The recent advancements in proteomics have become indispensable for diagnosing and understanding metabolic diseases like diabetes and obesity, while also significantly impacting pharmaceutical development.[13–15]

Enteroendocrine L-cells in the ileum primarily secrete glucagon-like peptide 1 (GLP-1) in response to food consumption.[16] GLP-1 exerts its effects by interacting with the GLP-1 receptor (GLP-1R), which shows widespread expression across various tissues, especially in the lung.[17] The drug Semaglutide, known for its prolonged effect on GLP-1 receptors, has received authorization to treat obesity in people, regardless of their type 2 diabetes status. It provides weight loss benefits and targets metabolic anomalies in obese people, alongside its hypoglycemic effects.[18,19] It has been demonstrated that GLP-1R agonists ameliorate experimental lung fibrosis.[20] Sodium-glucose transport protein 2 (SGLT2) inhibitors, emerging as novel oral hypoglycemic agents, effectively reduce blood glucose levels through the reduction of renal glucose reabsorption and enhancing urinary glucose excretion.[21] The administration of empagliflozin, an SGLT2 inhibitor, not only reduces mortality rates but also impedes the progression of experimental pulmonary hypertension.[22] Empagliflozin has demonstrated efficacy in combating airway hyperresponsiveness and fibrosis induced by obesity in a mouse model.[23]

This research investigated the impact of semaglutide, empagliflozin, and a high-fat diet on the expression of proteins in the lungs of a mouse model with obesity through proteomic techniques. Bioinformatics analysis was employed to delve deeper into the potential impacts of semaglutide and empagliflozin on the lungs of obese mice, providing novel perspectives and potential avenues for preventing and treating lung damage associated with obesity.

# Materials and Methods

## Animal Model

Six-week-old male C57BL/6JC mice were obtained from Hebei In Vivo Biotechnology Co., Ltd. and housed in the Hebei General Hospital's Experimental Animal Center. The incubation conditions included a temperature of 22°C ± 2°C, a humidity of 55% ± 10%, and a light/dark cycle of 12:12 hours. Throughout the trial, food and drink were freely available to each mouse.

Following a week-long period of acclimation, the animals were randomly divided into two groups using the random number table technique: a high-fat dietary feeding group (HFD group, n = 21) and a control feeding group (NCD group, n = 7). The control group's diet comprised 20% protein, 70% carbohydrates, and 10% fat, while the HFD group received a diet consisting of 20% protein, 20% carbohydrates, and 60% fat. The mice in each group were provided with the same caloric intake daily and had unlimited access to water. After 12 weeks on the high-fat diet, mice in the HFD group were screened for obesity, ensuring their body weight was equal to or greater than 20% of the average body weight of the control group. The HFD group was subsequently divided into three groups: the HFD group (n = 7), the HFD group with semaglutide (Sema group, n = 7), and the HFD group with empagliflozin (Empa group, n = 7). The Sema group received intraperitoneal administration of semaglutide at a dosage of 30 nmol/kg/day, while the Empa group received empagliflozin at a dosage of 10 mg/kg/day via gavage. Both NCD and HFD groups received an equivalent dosage intraperitoneally over 12 weeks. Dosage recommendations for semaglutide and empagliflozin were established using results from previously conducted research.[24–28] All experiments and procedures were conducted in accordance with the Regulations on the Management of Laboratory Animals issued by the National Science and Technology Commission and were approved by the Animal Ethics Association of the Hebei General Hospital (Approval Number: 2022–85; Date of approval: May 1, 2022). The ARRIVE criteria were adopted in all animal trials.

## Glucose Tolerance Tests

The Roche Blood Glucose Monitoring System was utilized to monitor blood glucose levels. After 12 weeks of semaglutide and empagliflozin treatment, a glucose tolerance test was conducted. Mice underwent an overnight fast

and received an intraperitoneal injection of 2 g of 50% glucose/kg body weight. Blood glucose levels from the tail vein were assessed at 0, 15, 30, 60, 90, and 120 minutes.

## Sample Collection and Preparation

Blood samples were taken from the eyes of the mice after an overnight fast and then spun in a centrifuge at 4°C for 10 minutes at a speed of 3,000 rpm to obtain the serum, which was stored at −80°C. Following blood collection, mice were euthanized, bilateral lung regions were swiftly isolated on an ice tray, and the lungs were assessed. Some lung tissues were preserved in 4% paraformaldehyde, while the remainder was preserved at −80°C.

## Serum Indicator Testing

Serum concentrations of low-density lipoprotein cholesterol (LDL-C), high-density lipoprotein cholesterol (HDL-C), total cholesterol (TC) and triglycerides (TG) were measured using a fully automated biochemical analyzer. Oxidative stress indicators, including malonaldehyde (MDA) and superoxide dismutase (SOD), were ascertained using ELISA.

## Histopathological Examination

Lung tissues were extracted bilaterally, weighed, and preserved in 4% paraformaldehyde for 48 h. Subsequently, tissues were dehydrated, wax-soaked, and embedded in paraffin blocks. Sections with a thickness of 3 to 5 μm underwent HE, Masson, and EVG staining. The Eclipse Ci-L photomicroscope (Nikon Eclipse E100) was used to select tissue-specific regions for imaging, ensuring coverage of the entire field of view and uniform background illumination in each photograph.

## Protein Extraction and TMT Labeling

Lung tissues were ground, and SDT buffer (4%SDS, 100 mM Tris-HCl, 1 mM DTT, pH 7.6) was used for lysis. UA buffer (8 M Urea, 150 mM Tris-HCl pH 8.0) was utilized to eliminate detergents, DTT, and other low molecular weight components from protein samples.[29] The solution underwent alkylation using 100 mL of iodoacetamide (100 mM IAA in UA buffer) for a duration of 30 minutes at ambient temperature in a dark environment. Subsequently, the protein underwent digestion using 4 mg trypsin (Promega) at a temperature of 37°C for an entire night, followed by the collection of the resultant peptides. TMT reagent labeled the peptide blend of 100 mg from every sample adhering to the instructions provided by the maker.

## Liquid Chromatography-Mass Spectrometry Mass Spectrometry Analysis (LC-MS/MS Analysis)

The procedure involved dissolving the samples in Buffer A (0.1% Formic acid) and B (84% acetonitrile and 0.1% Formic acid), followed by separation using a C18-reversed phase analytical column (Thermo Scientific Easy Column, 10 cm in length, 75 μm in inner diameter, 3μm resin).[30] Peptide analysis was performed using the Q Exactive mass spectrometer (Thermo Scientific) in conjunction with Easy nLC for a duration of 60 to 90 minutes. For acquiring MS data, the top10 beam-type CID fragmentation (HCD), which depends on data, was employed, and the MASCOT engine (Matrix Science, London, UK; version 2.2), incorporated into Proteome Discoverer 1.4 software, was utilized for identification and quantification.

## Screening of Differentially Expressed Proteins (DEPs)

The MASCOT Engine of Proteome Discoverer 1.4 software (Matrix Science, London, UK; version 2.2) thoroughly analyzed raw data. The acceptable range for peptide mass tolerance was ±20 ppm, with a fragment mass tolerance of 0.1Da and a false positive rate of 0.01 or lower. Bioinformatics methods were executed following previous literature.[31]

## GO and KEGG Analyses

The NCBI BLAST+ client software (ncbi-blast-2.2.28+-win32.exe) searched protein sequences of identified DEPs. The Blast2GO software (https://www.blast2go.com/) was utilized to conduct an enrichment analysis on gene ontology (GO) terms and annotate functions. The outcomes of GO annotations were charted utilizing R software. The KEGG database (https://www.kegg.jp/) was utilized to analyze the pathway annotations of DEPs. Enrichment analysis employed Fisher's exact test, whereas P-values were adjusted using the Benjamini–Hochberg method, setting the DEP screening threshold at $P < 0.05$.

## Statistical Analysis

GraphPad Prism 8.0 software was utilized for the statistical evaluations. Experimental data that conformed to a normal distribution were represented using mean values and standard deviation. The Tukey's test, following one-way ANOVA, analyzed multiple comparisons. Statistical significance was attributed to the observed disparities among the groups, possessing a *P*-value less than 0.05 for statistical significance.

# Results

## Body Weight and Lung Weight Variations in Four Distinct Groups

Initially, no substantial variations in body weight were observed among the four groups of mice. Yet, following a 12-week period of consuming a high-fat diet, the mice in the HFD group showed a substantial increase in body weight, over 20%, in contrast to those in the non-fat diet group, indicating the successful establishment of the obesity model. Over the 24 weeks, both the Sema and Empa groups experienced considerable drops in body weight compared to the HFD group, with the Sema group displaying a more pronounced decrease. From the seventeenth week onward, the Sema and NCD groups exhibited similar body weights ($P > 0.05$). Notably, the Sema group consistently had lower weights than the Empa group from week 18 onwards, and this difference was significant (Figure 1B) ($P < 0.05$). Figure 1A compares the morphological characteristics of mice across different groups at the end of the experiment, illustrating the body weight changes following high-fat, semaglutide, and empagliflozin treatments.

In terms of lung weights, HFD mice exhibited a corresponding increase compared to NCD mice ($P < 0.01$). However, lung weights were attenuated in both the Sema ($P < 0.001$) and Empa ($P < 0.05$) groups. No discernible variation in lung weights occurred following the administration of semaglutide and empagliflozin ($P > 0.05$) (Figure 1C).

## Changes in Blood Glucose and Lipid Levels Among Four Mouse Groups

Mice showed a marked rise in blood sugar levels due to changes in glucose tolerance. In comparison with the NCD, Sema, and Empa groups, blood glucose levels were significantly higher in the HFD group at 15, 30, 60, 90, and 120 min, peaking at 15 min and declining slowly. Blood glucose levels in the Sema and Empa groups rose slowly, peaked at 30 min, and then gradually declined, with no significant difference from those in the NCD group. Furthermore, the Sema and Empa groups did not demonstrate any noteworthy disparities in blood glucose levels ($P > 0.05$). These findings collectively indicate that both semaglutide and empagliflozin effectively lower blood glucose levels in the HFD-induced obesity mouse model (Figure 2A).

The HFD group exhibited elevated levels of TC ($P < 0.0001$), TG ($P < 0.01$), LDL-C ($P < 0.0001$), and HDL-C ($P < 0.0001$) in comparison to the NCD group. Comparing the sema groups to the HFD group, the levels of TC ($P < 0.001$), TG ($P < 0.01$), and LDL-C ($P < 0.05$) were considerably lower. However, there were no appreciable variations in HDL-C levels when contrasted with the HFD group. Differing from the HFD group, the Empa group exhibited a notable decrease in TC ($P < 0.001$) and LDL-C ($P < 0.001$), while there were no statistically significant alterations in HDL-C and TG levels ($P > 0.05$). Notably, there were no discernible variations between the Sema and Empa groups in their TC, TG, LDL-C, or HDL-C levels (Figure 2B–E) ($P > 0.05$).

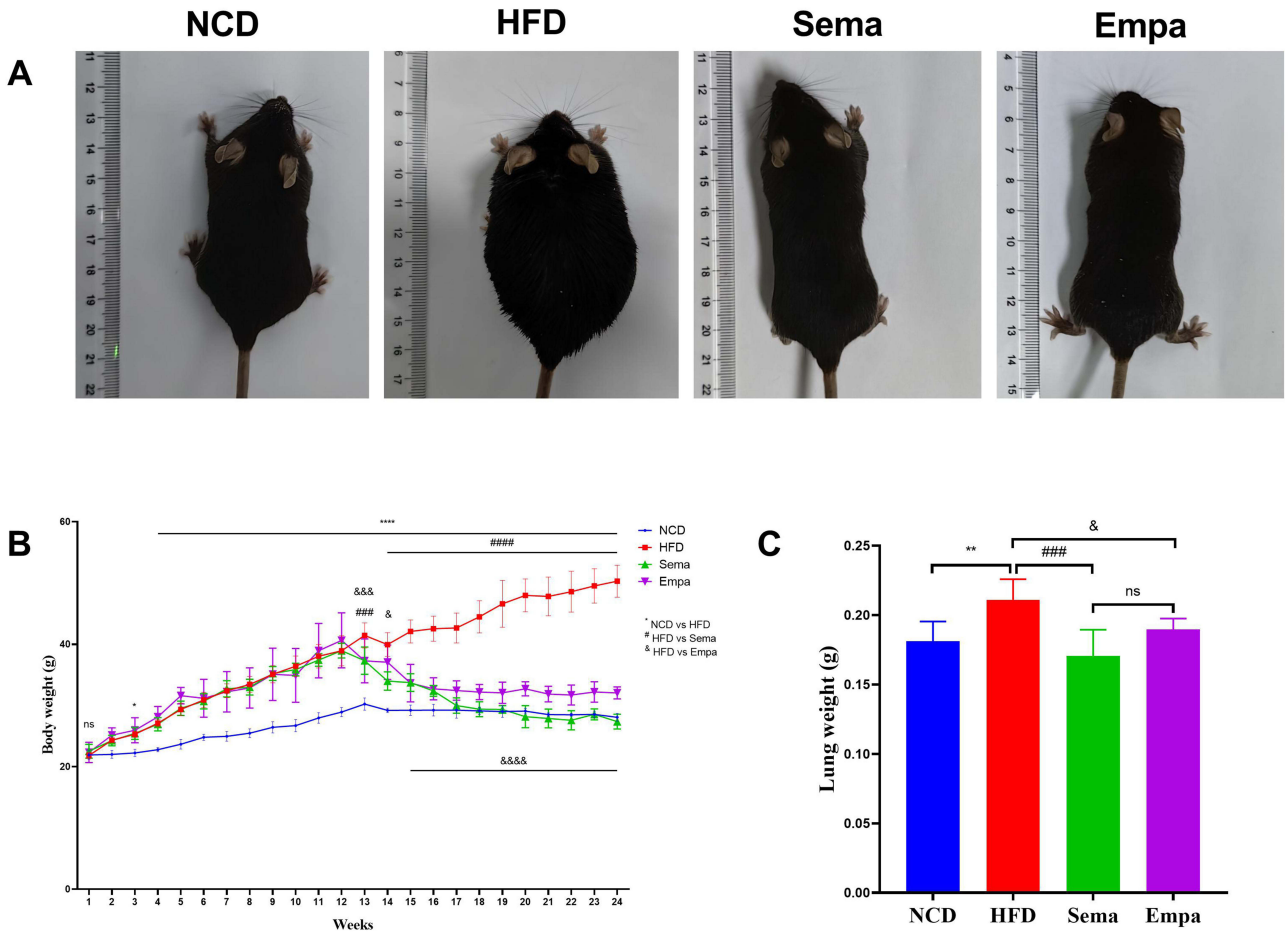


**Figure 1** (**A**) Visual representations of standard mice, mice with obesity, those treated with semaglutide, and mice treated with empagliflozin. (**B**) Observations of body weight fluctuations in mice across NFD, HFD, Sema, and Empa groups. (**C**) Changes in lung weight of four different mice groups. "ns"$P \geq 0.05$, *$P < 0.05$, **$P < 0.01$, ****$P < 0.0001$ NCD vs HFD, $^{\#\#\#\#}P < 0.001$, $^{\#\#\#\#\#}P < 0.0001$ HFD vs Sema, $^{\&}P < 0.05$, $^{\&\&\&}P < 0.001$, $^{\&\&\&\&}P < 0.0001$ HFD vs Empa.

## Semaglutide and Empagliflozin Affect Serum Oxidative Stress Indices in Obese Mice

To elucidate variations in serum oxidative stress levels among the four groups, pro- and anti-oxidative stress molecules, SOD, and MDA, were assessed. Observations revealed a notable decrease in SOD levels ($P < 0.0001$), while MDA concentrations were markedly enhanced ($P < 0.001$) in HFD mice compared to NCD mice (Figure 3A and B). Serum SOD and MDA concentrations in both Sema and Empa mice were significantly higher and lower, respectively than in HFD animals (all $P < 0.05$). These findings suggest that a prolonged high-fat diet induces excessive oxidative stress, a condition mitigated by exogenous administration of semaglutide and empagliflozin. Significantly, the Empa and Sema groups exhibited no substantial differences ($P > 0.05$).

## Pulmonary Pathological Changes

H&E staining results indicated that HFD mice exhibited thickened alveolar walls, reduced alveolar lumen, and enlarged interstitial spaces between alveoli compared to NCD mice. Conversely, the alveolar morphology of both Sema and Empa mice was significantly improved compared to HFD mice (Figure 4A and B). Masson's staining revealed increased collagen deposition in HFD mice compared to Sema, Empa, and NCD mice, potentially impacting lung compliance and leading to fibrosis and lung failure (Figure 4C and D).

EVG staining highlighted blue and black elastic fibers, proliferation, cracking, and disintegration in the HFD group, all of which were mitigated by semaglutide and empagliflozin administration (Figure 4E).

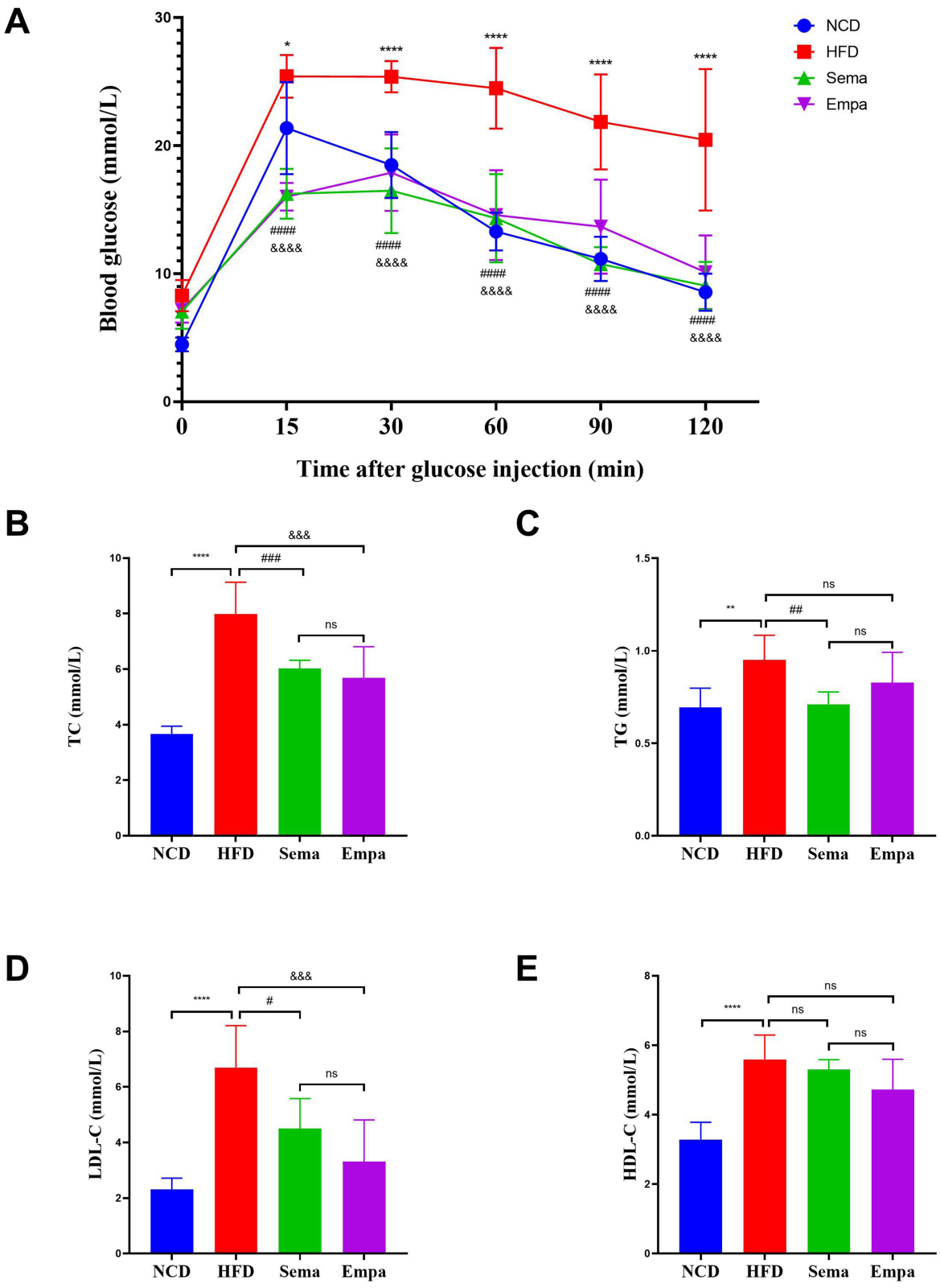


**Figure 2** (**A**) Glucose tolerance was determined by the IPGTT test. Comparison of TC (**B**), TG (**C**), LDL (**D**), HDL (**E**) among the four groups (n =7). "ns" $P \geq 0.05$, $^{*}P < 0.05$, $^{**}P < 0.01$, $^{****}P < 0.0001$ NCD vs HFD, $^{\#}P < 0.05$, $^{\#\#}P < 0.01$, $^{\#\#\#}P < 0.001$, $^{\#\#\#\#}P < 0.0001$ HFD vs Sema, $^{\&\&\&}P < 0.001$, $^{\&\&\&\&}P < 0.0001$ HFD vs Empa.

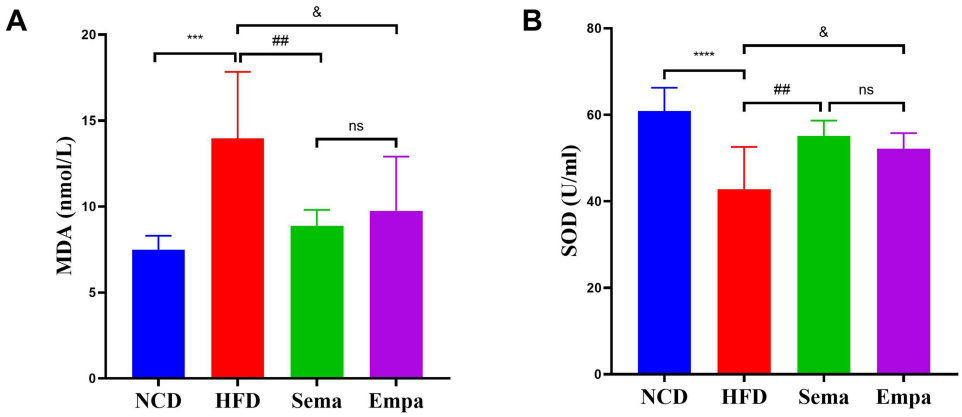


**Figure 3** Comparison of MDA (**A**) and SOD (**B**) in the indicated groups, (n =7).“ns”$P \geq 0.05$, ***$P < 0.001$, ****$P < 0.0001$ NCD vs HFD, $^{\#\#}P < 0.01$ HFD vs Sema, $^{\&}P < 0.05$ HFD vs Empa.

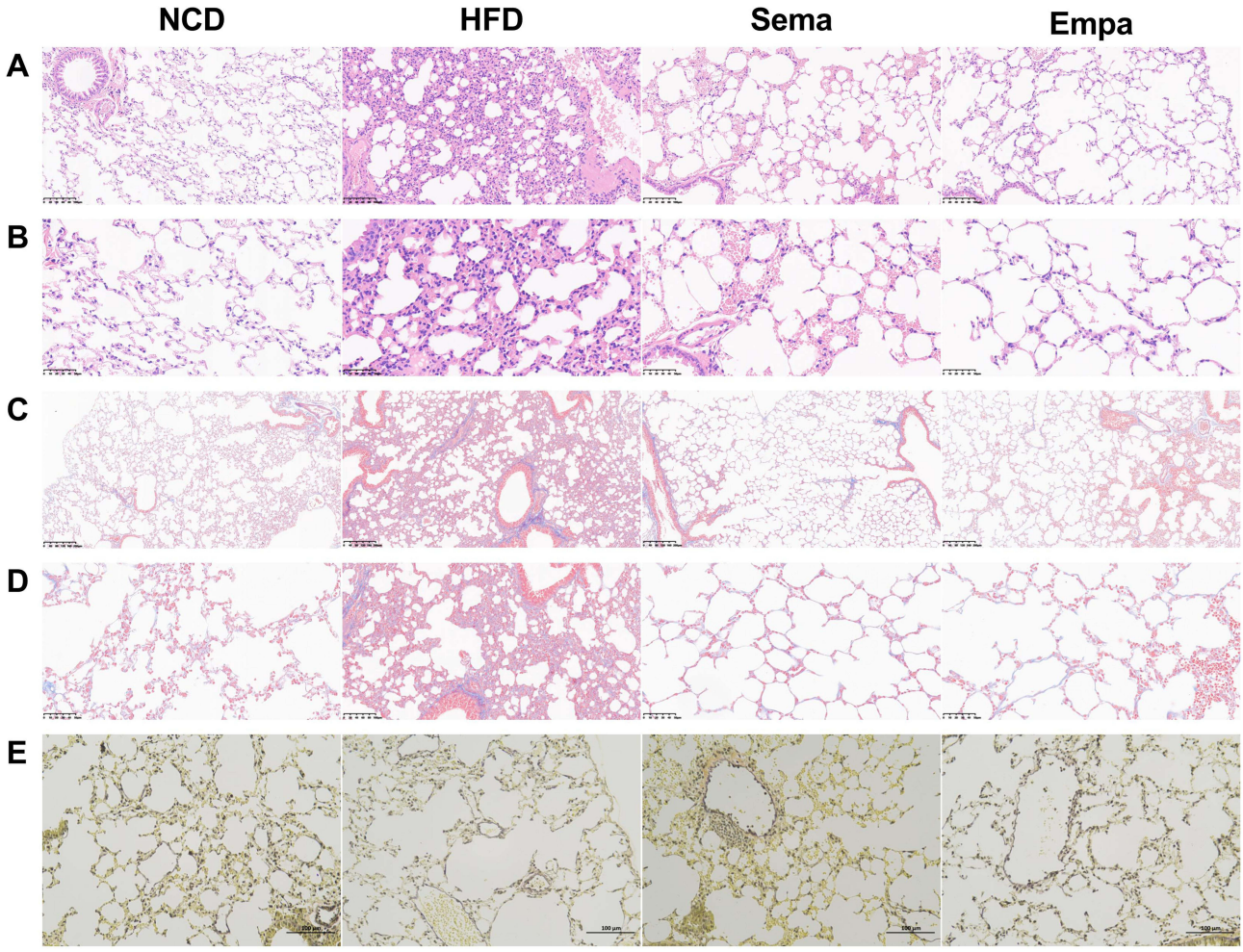


**Figure 4** Images using H&E staining on lung tissues from four distinct groups, featuring scale bars measuring 100 μm (**A**) and 50 μm (**B**). Images of lung tissues from four distinct groups, stained with Masson’s trichrome, featuring scale bars at 100 μm (**C**) and 50 μm (**D**). Representative EVG staining images of lung tissue of 4 different groups with scale bars at 100 μm (**E**).

## LC-MS/MS Analysis

Through LC-MS/MS analysis, 581,233 spectrum proteins, 83,023 matched-spectrum proteins, 38,242 peptides, 34,186 unique peptides, 5806 identified proteins, and 5804 quantified proteins were discovered (Figure 5A). Based

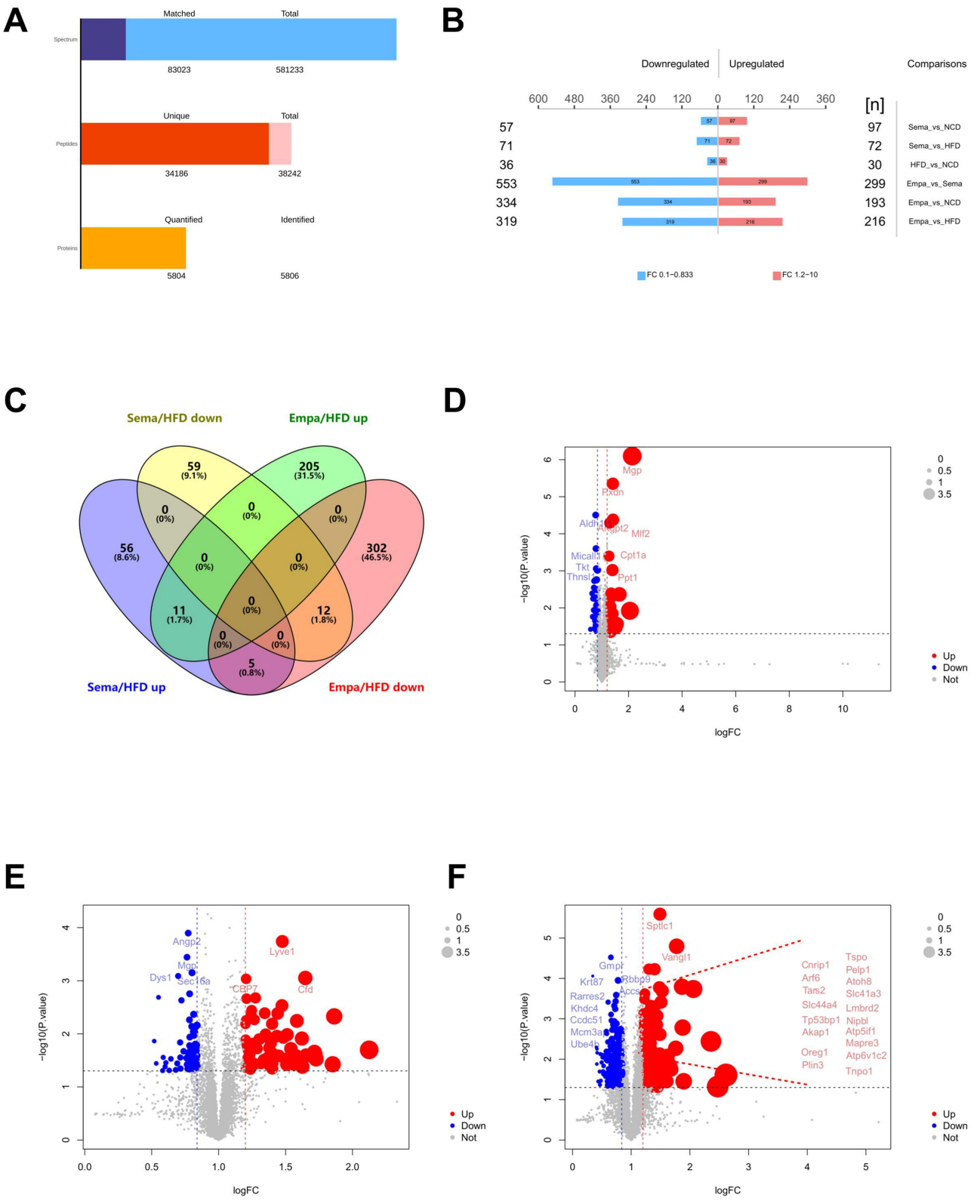


**Figure 5** (**A**) Results of LC-MS/MS analysis. (**B**) DEPs compared between the 4 groups. (**C**) The Venn diagram indicates the number of enhanced and reduced-regulated proteins between the Sema/HFD and Empa/HFD groups. (**D**–**F**) Volcano plots of DEPs. Blue markers represent proteins with reduced differential expression, red markers show proteins with increased differential expression, and grey markers denote proteins with no significant differential expression.

on prior studies, proteins exhibiting a fold change (FC) exceeding 1.2 and a *P* value below 0.05 were identified as DEPs.[32]

In the HFD/NCD group, there were 66 DEPs, comprising 30 proteins that were increased and 36 that were decrease. The Sema/HFD group yielded 143 DEPs, with 72 proteins being up-regulated and 71 proteins being down-regulated. Within the Empa/HFD group, there were 535 DEPs, out of which 216 proteins exhibited up-regulation while 319 proteins displayed down-regulation. The Empa/Sema group had 852 DEPs, with 299 proteins being up-regulated and 553 proteins being down-regulated (Figure 5B). The Venn diagram illustrated that Sema/HFD and Empa/HFD shared 23 overlapping DEPs, with 11 up-regulated and 12 down-regulated proteins simultaneously (Figure 5C). The volcano plot graphically represented the DEPs of HFD/NCD, Sema/HFD, and Empa/HFD (Figure 5D–F).

## GO Enrichment Analysis

GO analysis was performed at the cellular composition (CC), molecular function (MF), and biological processes (BP) levels. At the BP level, HFD/NCD mice exhibited alternative pathways and complement activation (Figure 6A). In contrast, the Sema/HFD groups primarily engaged in oxidative phosphorylation processes (Figure 6B), and the Empa/HFD mice demonstrated signaling and interaction between SA node cells and atrial myocardial cells (Figure 6C). At the MF level, the three groups of DEPs primarily manifested activity and binding functions (Figure 6D–F). The Cellular Component (CC) analysis revealed the respiratory chain as the predominant structural component in the Sema/HFD groups (Figure 6H), while the Empa/HFD group exhibited abundance in the SUMO ligase complex and the Smc5-Smc6

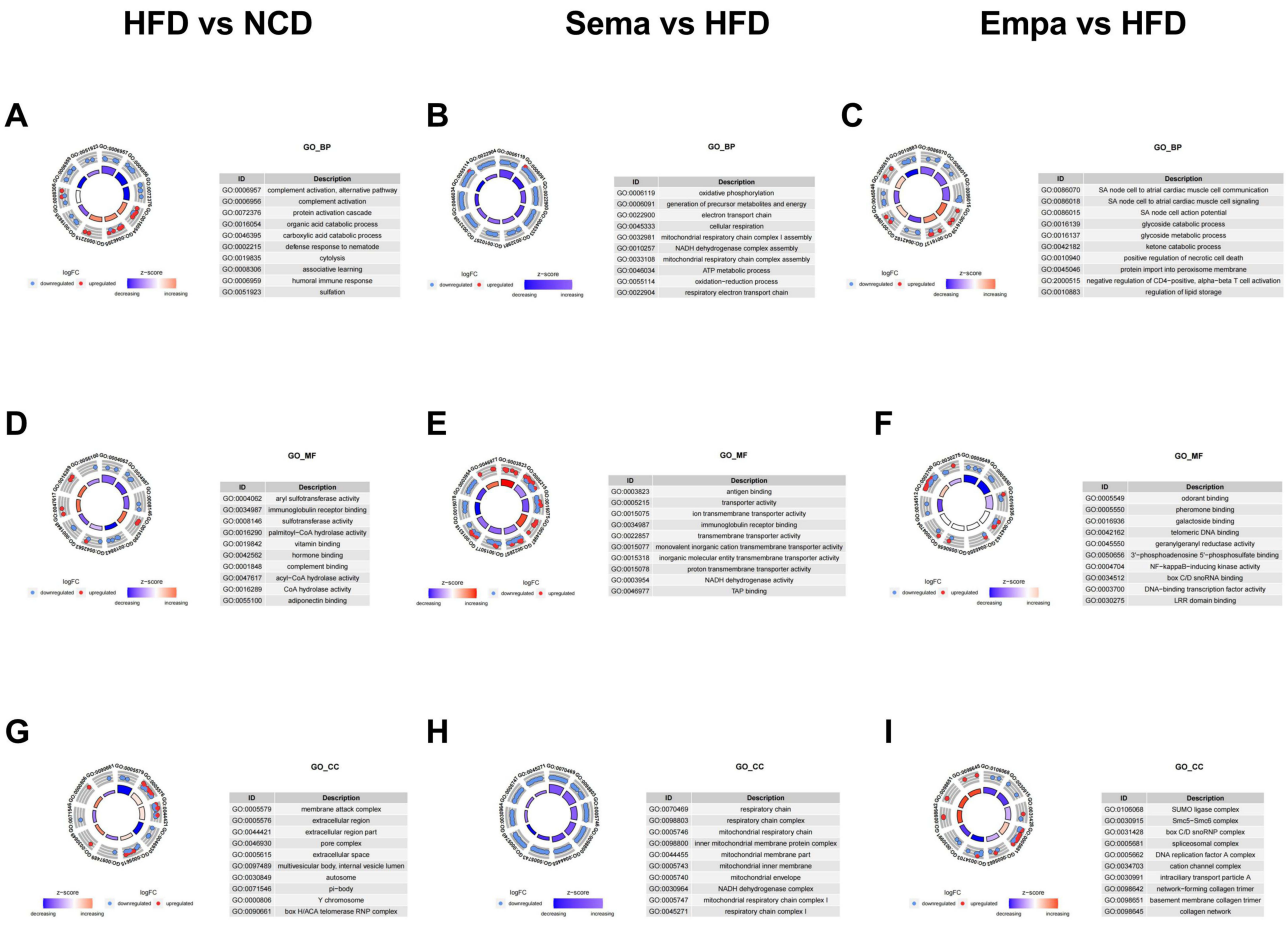


**Figure 6** (**A**) Biological process in HFD vs NCD. (**B**) Biological process in Sema vs HFD. (**C**) Biological process in Empa vs HFD. (**D**) Cellular component in HFD vs NCD. (**E**) Cellular component in Sema vs HFD. (**F**) Cellular component in Empa vs HFD. (**G**) Molecular function in HFD vs NCD. (**H**) Molecular function in Sema vs HFD. (**I**) Molecular function in Empa vs HFD.

complex (Figure 6I). In contrast, the membrane attack complex and the extracellular region were prominent structural components in the HFD/NCD groups (Figure 6G).

## KEGG Pathway Analysis

The KEGG database, a widely used public resource for studying cellular protein pathways, was employed to identify DEPs in the HFD/NCD, Sema/HFD, and Empa/HFD groups. The analysis revealed that DEPs in the HFD/NCD group had an impact on actin cytoskeleton regulation, asthma, complement and coagulation cascades, steroid biosynthesis, and fatty acid elongation (Figure 7A). Conversely, the Sema/HFD group showed distinct protein expression patterns associated with diabetic cardiomyopathy, oxidative phosphorylation, thermogenesis, and chemical carcinogenesis-reactive oxygen species (Figure 7B). In the Empa/HFD group, proteins were primarily enriched in folate biosynthesis, glycosaminoglycan degradation, pentose and glucuronate interconversions, and asthma (Figure 7C).

## Analysis of DEPs in Different Groups

To further explore the mechanism by which semaglutide and empagliflozin affect lung function, we analyzed DEPs from the HFD/NCD, Sema/HFD, Empa/HFD, and Sema/Empa groups. Initially, DEPs in the HFD/NCD and Sema/HFD groups were identified based on the principle of opposite direction (ie, proteins upregulated in the HFD/NCD group and downregulated in the Sema/HFD group, or vice versa), resulting in the identification of 12 target proteins (Table 1). Within the HFD/NCD cohort, there was a decrease in 15 proteins, which increased in Empa/HFD, whereas 7 proteins rose in HFD/NCD but decreased in Empa/HFD group (Table 2). Furthermore, the Sema/HFD and Empa/HFD groups exhibited elevated levels of 11 of the 23 proteins, in contrast to a reduction in 12 proteins (refer to Table 3).

Combining the results of the DEPs revealed an interesting finding: four proteins - lymphatic vessel endothelial hyaluronic acid receptor 1 (LYVE1), serine/threonine protein kinase B-raf (BRAF), regulator of cell cycle RGCC (RGCC), and charged multivesicular body protein 5 (CHMP5) - were downregulated when comparing the HFD group to the NCD group and reversed by semaglutide and empagliflozin treatment.

# Discussion

Numerous comorbidities, such as hypertension, diabetes, cardiovascular disease, renal insufficiency, and cancer, are associated with obesity, incurring significant financial costs.[33,34] Previous studies have indicated that obesity can induce fibrosis, bronchoconstriction, and hyperresponsive airways by disrupting insulin signaling.[35,36] A connection between nutrition-induced obesity and lung fibrosis has been established.[11] The presence of GLP-1R in various lung tissue regions, including alveolar type II (ATII) cells, pulmonary arterial smooth muscle, and tracheal submucosal glands has been reported.[37] The activation of GLP-1R is crucial for lung function under both normal and pathological conditions, as evidenced by its role in triggering the secretion of phosphatidylcholine in cultured ATII cells in vitro.[38,39] Additionally, the GLP-1R agonist liraglutide has demonstrated remarkable effectiveness in restoring lung function and reversing right ventricular hypertrophy by influencing pulmonary angiotensin-converting enzyme (ACE) and ACE2 expression, as well as surfactant protein (SP)-A and SP-B levels.[40] Semaglutide attenuates acute lung injury via blocking the HDAC5/NF-κB pathway.[41] Recent research has suggested that semaglutide possesses both anti-inflammatory and anti-apoptotic properties.[42] Empagliflozin, an SGLT2 inhibitor, not only reduces mortality rates but also impedes the advancement of experimental pulmonary hypertension.[22] It alleviates pulmonary fibrosis induced by bleomycin in rats through the modulation of Sesn2/AMPK/Nrf2 signaling and the regulation of ferroptosis and autophagy.[43] Empagliflozin has demonstrated efficacy in combating airway hyperresponsiveness and fibrosis caused by obesity in a mouse model.[23] Its application in the treatment of acute lung injury holds promise for advantageous outcomes and potential clinical applications.[44] Empagliflozin safeguards against pulmonary ischemia/reperfusion injury through a mechanism dependent on extracellular signal regulation of kinase 1 and 2.[45] Empagliflozin has been shown to have anti-fibrotic and anti-inflammatory properties in a number of organ fibrosis models without diabetes.[46,47] Moreover, empagliflozin has been shown to diminish inflammatory markers and oxidative stress within the lungs of mice, effectively averting pulmonary fibrosis.[48] Yet, at present, no research has been published regarding the impact of semaglutide and empagliflozin on lung damage associated with obesity.

**A**

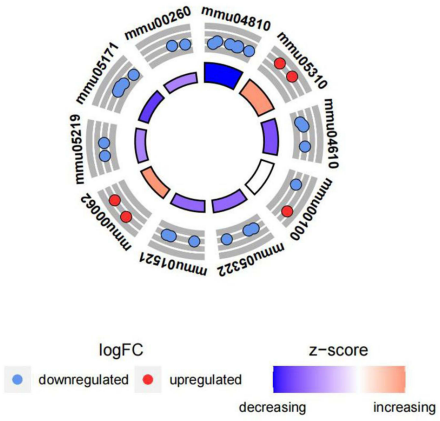


**KEGG**

| ID | Description |
|---|---|
| mmu04810 | Regulation of actin cytoskeleton |
| mmu05310 | Asthma |
| mmu04610 | Complement and coagulation cascades |
| mmu00100 | Steroid biosynthesis |
| mmu05322 | Systemic lupus erythematosus |
| mmu01521 | EGFR tyrosine kinase inhibitor resistance |
| mmu00062 | Fatty acid elongation |
| mmu05219 | Bladder cancer |
| mmu05171 | Coronavirus disease − COVID−19 |
| mmu00260 | Glycine, serine and threonine metabolism |

**B**

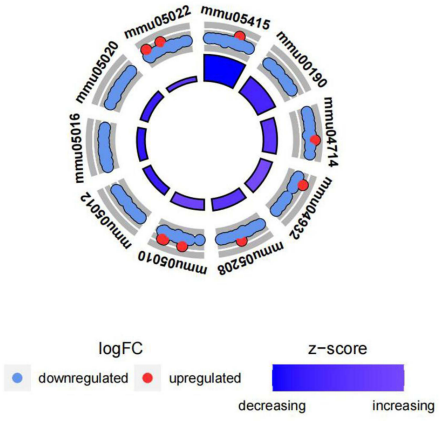


**KEGG**

| ID | Description |
|---|---|
| mmu05415 | Diabetic cardiomyopathy |
| mmu00190 | Oxidative phosphorylation |
| mmu04714 | Thermogenesis |
| mmu04932 | Non−alcoholic fatty liver disease |
| mmu05208 | Chemical carcinogenesis − reactive oxygen species |
| mmu05010 | Alzheimer disease |
| mmu05012 | Parkinson disease |
| mmu05016 | Huntington disease |
| mmu05020 | Prion disease |
| mmu05022 | Pathways of neurodegeneration − multiple diseases |

**C**

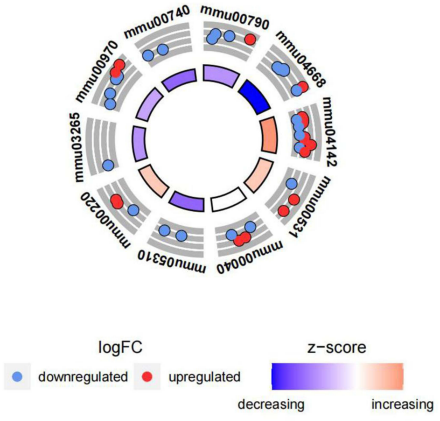


**KEGG**

| ID | Description |
|---|---|
| mmu00790 | Folate biosynthesis |
| mmu04668 | TNF signaling pathway |
| mmu04142 | Lysosome |
| mmu00531 | Glycosaminoglycan degradation |
| mmu00040 | Pentose and glucuronate interconversions |
| mmu05310 | Asthma |
| mmu00220 | Arginine biosynthesis |
| mmu03265 | Virion − Lyssavirus |
| mmu00970 | Aminoacyl−tRNA biosynthesis |
| mmu00740 | Riboflavin metabolism |

**Figure 7** KEGG enrichment analysis of DEPs between (**A**) HFD/NCD, (**B**) Sema/HFD, and (**C**) Empa/HFD groups.

This investigation observed a significant reduction in body and lung weight in obese mice following semaglutide and empagliflozin treatment. Interestingly, starting in week 18, the body weights of mice following semaglutide administration were significantly lower than those following empagliflozin intervention. This study found that mice on a high-fat

**Table 1** Comparison of DEPs Between HFD/NCD and Sema/HFD Groups

| Accession | Protein Name | Gene Name | HFD/NCD | Sema/HFD |
|---|---|---|---|---|
| P19788 | Matrix Gla protein | Mgp | Up | Down |
| O35608 | Angiopoietin-2 | Angpt2 | Up | Down |
| P50544 | Very long-chain specific acyl-CoA dehydrogenase, mitochondrial | Acadvl | Up | Down |
| P56394 | Cytochrome coxidase copper chaperone | Cox17 | Up | Down |
| Q8K211 | High affinity copper uptake protein 1 | Slc31a1 | Down | Up |
| Q9DBX1 | Regulator of cell cycle | Rgcc | Down | Up |
| P28028 | Serine/threonine-protein kinase B-raf | Braf | Down | Up |
| P03987 | Ig gamma-3 chain C region | | Down | Up |
| Q9D7S9 | Charged multivesicular body protein 5 | Chmp5 | Down | Up |
| Q8BHC0 | Lymphatic vessel endothelial hyaluronic acid receptor 1 | Lyve1 | Down | Up |
| Q8VCN5 | Cystathionine gamma-lyase | Cth | Down | Up |
| P03953 | Complement factor D | Cfd | Down | Up |

**Table 2** Comparison of DEPs Between HFD/NCD and Empa/HFD Groups

| Accession | Protein Name | Gene Name | HFD/NCD | Empa/HFD |
|---|---|---|---|---|
| Q99L60 | V-type proton ATPase subunit C 2 | Atp6v1c2 | Down | Up |
| Q3V038 | Tetratricopeptide repeat protein 9A | Ttc9 | Down | Up |
| Q9DBX1 | Regulator of cell cycle RGCC | Rgcc | Down | Up |
| Q80T21 | ADAMTS-like protein 4 | Adamtsl4 | Down | Up |
| Q9D0J8 | Parathymosin | Ptms | Down | Up |
| Q99MV1 | Tudor domain-containing protein 1 | Tdrd1 | Down | Up |
| P28028 | Serine/threonine-protein kinase B-raf | Braf | Down | Up |
| Q9R1Q7 | Proteolipid protein 2 | Plp2 | Down | Up |
| Q9D7S9 | Charged multivesicular body protein 5 | Chmp5 | Down | Up |
| Q8BHC0 | Lymphatic vessel endothelial hyaluronic acid receptor 1 | Lyve1 | Down | Up |
| P52840 | Sulfotransferase 1A1 | Sult1a1 | Down | Up |
| P60824 | Cold-inducible RNA-binding protein | Cirbp | Down | Up |
| P20065 | Thymosin beta-4 | Tmsb4x | Down | Up |
| Q9Z2C4 | Myotubularin-related protein 1 | Mtmr1 | Down | Up |
| P01878 | Ig alpha chain C region | | Down | Up |
| Q3U186 | Probable arginine–tRNA ligase, mitochondrial | Rars2 | Up | Down |
| P12710 | Fatty acid-binding protein, liver | Fabp1 | Up | Down |
| Q61878 | Bone marrow proteoglycan | Prg2 | Up | Down |
| Q5FW60 | Major urinary protein 20 | Mup20 | Up | Down |
| P49290 | Eosinophil peroxidase | Epx | Up | Down |
| Q3TCX3 | KH homology domain-containing protein 4 | Khdc4 | Up | Down |
| Q62141 | Paired amphipathic helix protein Sin3b | Sin3b | Up | Down |

diet exhibited increased levels of TC, TG, LDL-C, and HDL-C compared to those on a non-fat diet. The Sema and Empa groups demonstrated a decrease in TC and LDL-C levels following the administration of semaglutide and empagliflozin, in contrast to the HFD. Hence, both semaglutide and empagliflozin improved the weight and lipid metabolism of obese mice, aligning with the findings from earlier research.[24,26,49] Furthermore, both semaglutide and empagliflozin effectively reduced blood glucose levels in the HFD-induced obesity mouse model. This suggests that the combined use of these two drugs could enhance the pronounced effect of lowering blood sugar, blood lipids, and inducing weight loss.

These outcomes were further confirmed through histological examination using H&E staining. The lung tissues of HFD mice exhibited increased alveolar wall thickness, narrowing of alveolar lumens, and the accumulation of adipocytes compared to the NCD group. After intervention with semaglutide and empagliflozin, both groups of mice demonstrated changes in lung

**Table 3** Comparison of DEPs Between Sema/HFD and Empa/HFD Groups

| Accession | Protein Name | Gene Name | Sema/HFD | Empa/HFD |
|---|---|---|---|---|
| P08122 | Collagen alpha-2(IV) chain | Col4a2 | Up | Up |
| Q9QZ85 | Interferon-inducible GTPase 1 | Iigp1 | Up | Up |
| P02463 | Collagen alpha-1(IV) chain | Col4a1 | Up | Up |
| Q61092 | Laminin subunit gamma-2 | Lamc2 | Up | Up |
| Q8BHC0 | Lymphatic vessel endothelial hyaluronic acid receptor 1 | Lyve1 | Up | Up |
| Q9D7S9 | Charged multivesicular body protein 5 | Chmp5 | Up | Up |
| O88668 | Protein CREG1 | Creg1 | Up | Up |
| O35704 | Serine palmitoyltransferase 1 | Sptlc1 | Up | Up |
| P28028 | Serine/threonine-protein kinase B-raf | Braf | Up | Up |
| Q91YL2 | E3 ubiquitin-protein ligase RNF126 | Rnf126 | Up | Up |
| Q9DBX1 | Regulator of cell cycle RGCC | Rgcc | Up | Up |
| Q8C138 | Androgen-dependent TFPI-regulating protein | Adtrp | Down | Down |
| Q80U30 | Protein CLEC16A | Clec16a | Down | Down |
| Q62147 | Sarcospan | Sspn | Down | Down |
| P02762 | Major urinary protein 6 | Mup6 | Down | Down |
| Q3URS9 | Mitochondrial potassium channel | Ccdc51 | Down | Down |
| Q3UIU2 | NADH dehydrogenase [ubiquinone] 1 beta subcomplex subunit 6 | Ndufb6 | Down | Down |
| Q8VD57 | Vesicle transport protein SFT2B | Sft2d2 | Down | Down |
| O89090 | Transcription factor Sp1 | Sp1 | Down | Down |
| Q9ESD7 | Dysferlin | Dysf | Down | Down |
| Q6IMF0 | Keratin, type II cuticular 87 | Krt87 | Down | Down |
| O54692 | Centromere/kinetochore protein zw10 homolog | Zw10 | Down | Down |
| Q69ZR9 | Protein TASOR | Tasor | Down | Down |

structure, characterized by a decrease in alveolar wall thickness and enlargement of the alveolar lumen. Collagen deposition was higher in HFD mice than in Sema, Empa, or NCD mice, and elastic fibers proliferated, cracked, and disintegrated according to Masson and EVG staining. This finding is consistent with other research suggesting that an HFD may aggravate pulmonary fibrosis.[50] It also implies that obesity may lower lung compliance, potentially leading to lung collapse, pulmonary fibrosis, or even lung failure. Empagliflozin and semaglutide show promise in treating this disease.

Obese HFD mice had notably decreased SOD levels and significantly increased MDA levels compared to NCD mice; this effect was reversed after semaglutide and empagliflozin treatment. These data suggest that in chronic HFD mice, there is elevated oxidative stress, and exogenous semaglutide and empagliflozin treatment can regulate and alleviate this stress. According to our study, both semaglutide and empagliflozin protect the lungs by reducing oxidative stress, and combining the two drugs may amplify this beneficial effect.

In this study, proteomic methods were employed to investigate the proteome expression patterns of lung tissue from mice that were healthy, obese, treated with semaglutide, and treated with empagliflozin. Subsequently, we used bioinformatics methodologies to unveil the characteristics of DEPs, laying the groundwork for ultimately screening proteins associated with obesity-related pulmonary dysfunction. Combining the data from the DEPs led to an intriguing discovery: four proteins were downregulated in the high-fat diet group compared to the NCD group, and this effect was reversed by treatment with semaglutide and empagliflozin. These proteins are LYVE1, BRAF, RGCC and CHMP5.

In recent studies, the protein RGCC, also known as the response gene to complement 32 (RGC-32), has been identified as a novel profibrotic factor in renal function.[51] It safeguards against pulmonary fibrosis, and reducing it leads to the buildup of collagen. Consequently, reinstating RGCC expression could hold therapeutic promise in combating pulmonary fibrosis.[52] Here, it was observed that an HFD dramatically reduced RGCC expression, which was significantly increased by semaglutide and empagliflozin. Therefore, it is presumed that semaglutide and empagliflozin exert a potential lung protective function by regulating RGCC protein expression.

LYVE1, a receptor located in the lymphatic system, facilitates angiogenesis through the interplay between lymphatic and blood endothelial cells.[53] The primary expression of LYVE1 occurs in the endothelial cells of lymphatic capillaries.[54,55] The LYVE1 molecule is considered the primary immunohistochemical marker of lymphatic endothelial cells.[56] Altered expression of LYVE1 has been demonstrated to impair lymphatic transport function.[57] The lymphatic vasculature significantly contributes to maintaining lung homeostasis by eliminating immune cells and draining interstitial fluid.[58–60] LYVE1 has been implicated in lung diseases, with LYVE1 gene expression significantly reduced in COPD and lung adenocarcinoma, suggesting a possible molecular link between these pathological conditions.[61] Serum LYVE1 appears to decrease in metastatic lung cancer.[62] Inflammatory stimuli can lead to decreased surface expression of LYVE1.[63] As far as we are aware, this research is pioneering in suggesting that obesity caused by a high-fat diet could impact pulmonary health by diminishing LYVE1 expression, which is believed to be linked to lymphatic transport and angiogenesis. Semaglutide and empagliflozin have the potential to enhance lung function by significantly boosting the expression of LYVE1 in the lungs of obese mice, found on the surface of lymphatic endothelial cells and essential for lymphatic transport and growth.

BRAF, a serine/threonine protein kinase located on chromosome 7q34, can activate the MAPK/ERK-signaling pathway. MAPK, belonging to the serine-threonine kinases superfamily, may participate in the development of various illnesses.[64] Accumulating evidence indicates that the MAPK signaling pathway can promote lung fibroblasts activation and the accumulation of extracellular matrix.[65,66] Research indicates that the MAPK/ERK pathway plays a role in controlling lung mesenchyme, which in turn impacts its growth.[67] Activation of the MAPK/ERK pathway facilitates embryonic development, contributes to various physiological processes including growth, differentiation, survival, migration, and morphogenesis.[68,69] Our proposition is that obesity negatively impacts lung function and damages lung structure via the MAPK/ERK signaling pathway. Conversely, both semaglutide and empagliflozin enhanced lung health by upregulating BRAF protein expression and modulating the MAPK/ERK pathway, thereby preventing pulmonary fibrosis and mitigating inflammation.

As a coiled protein, CHMP5 aids in converting the late endosomal multivesicular body into lysosomes.[70,71] Disruption of the mouse CHMP5 gene may lead to the deregulation of signaling pathways such as NF-κB and TGF β (transforming growth factor β).[71] Additionally, there was a notable rise in CHMP5 levels in acute leukemia cases, suggesting its potential involvement in leukemogenesis.[72] Currently, there are no publications related to the lung health and the CHMP5 protein.

The majority of type 2 diabetes sufferers will ultimately require the combination of multiple antidiabetic drugs for effective glycemic management. Previous studies have investigated that once-weekly treatment with semaglutide and empagliflozin achieves a significant reduction in HbA1c and can improve glycemic control and plasma aldosterone levels.[73,74] The American Diabetes Association (ADA) and the European Association for the Study of Diabetes (EASD) collectively advise using SGLT2 inhibitors or GLP-1R agonists for type 2 diabetes patients with a heightened risk of cardiovascular incidents.[75] Combination treatment of empagliflozin and semaglutide may offer additional cardiovascular protection in patients with type 2 diabetes.[76] In our study, obesity increases the levels of lipids, glucose and oxidative stress in blood, resulting in impaired lung structure. Treatment with semaglutide and empagliflozin improved lipid metabolism, reduced oxidative stress and protected lung function. Combined use of semaglutide and empagliflozin may result in therapeutic effects in obesity-induced lung injury enhanced effects. While the exact processes driving the combined or synergistic impacts remain elusive, altering the levels of LYVE1, BRAF, RGCC, and CHMP5 in the lung tissues of obese mice, as noted, might contribute to the understanding.

This study has certain limitations. Initially, the joint use of semaglutide and empagliflozin in treating lung damage associated with obesity was not investigated. We think that the combination might be more effective than the single drug, but more research is needed to confirm this. Additionally, no measurements were taken regarding lung function.

## Conclusion

In summary, this study demonstrates obesity induced by a high-fat diet causes a reduction in the expression of LYVE1, BRAF, RGCC, and CHMP5 proteins, potentially affecting the lung function and structure in mice. Significantly, the administration of semaglutide and empagliflozin elevates the levels of these proteins, potentially offering therapeutic

benefits against lung injury caused by obesity. Merging semaglutide with empagliflozin may exert a more pronounced impact.

## Data Sharing Statement

Data supporting the findings of this study are available from the corresponding authors.

Reasonable request.

## Ethics Statement

All experiments and procedures were conducted in accordance with the Regulations on the Management of Laboratory Animals issued by the National Science and Technology Commission and were approved by the Animal Ethics Association of the Hebei General Hospital (Approval Number: 2022-85; Date of approval: May 1,2022). The ARRIVE criteria were adopted in all animal trials.

## Funding

This study was supported by the Hebei Province Natural Science Foundation (206Z7702G, 22377713D and H2022307026). The funding bodies were not involved in the design of the study and collection, analysis, and interpretation of data and in writing the manuscript.

## Disclosure

The authors report no conflicts of interest in this work.

## References

1. Ponasenko A, Sinitsky M, Minina V, et al. Immune response and lipid metabolism gene polymorphisms are associated with the risk of obesity in middle-aged and elderly patients. *J Pers Med*. 2022;12(2):238. doi:10.3390/jpm12020238
2. Lustig RH, Collier D, Kassotis C, et al. Obesity I: overview and molecular and biochemical mechanisms. *Biochem Pharmacol*. 2022;199:115012. doi:10.1016/j.bcp.2022.115012
3. Watson RA, Pride NB, Thomas EL, et al. Reduction of total lung capacity in obese men: comparison of total intrathoracic and gas volumes. *J Appl Physiol*. 2010;108(6):1605–1612. doi:10.1152/japplphysiol.01267.2009
4. Behazin N, Jones SB, Cohen RI, Loring SH. Respiratory restriction and elevated pleural and esophageal pressures in morbid obesity. *J Appl Physiol*. 2010;108(1):212–218. doi:10.1152/japplphysiol.91356.2008
5. Jones RL, Nzekwu M-MU. Nzekwu MM.The effects of body mass index on lung volumes. *Chest*. 2006;130(3):827–833. doi:10.1378/chest.130.3.827
6. Sharp JT, Henry JP, Sweany SK, Meadows WR, Pietras RJ. The total work of breathing in normal and obese men. *J Clin Invest*. 1964;43(4):728–739. doi:10.1172/JCI104957
7. Young T, Skatrud J, Peppard PE. Risk factors for obstructive sleep apnea in adults. *JAMA*. 2004;291(16):2013–2016. doi:10.1001/jama.291.16.2013
8. Mokhlesi B, Kryger MH, Grunstein RR. Assessment and management of patients with obesity hypoventilation syndrome. *Proc Am Thorac Soc*. 2008;5(2):218–225. doi:10.1513/pats.200708-122MG
9. Beuther DA, Sutherland ER. Overweight, obesity, and incident asthma: a meta-analysis of prospective epidemiologic studies. *Am J Respir Crit Care Med*. 2007;175(7):661–666. doi:10.1164/rccm.200611-1717OC
10. Lambert AA, Putcha N, Drummond MB, et al. Obesity is associated with increased morbidity in moderate to severe COPD. *Chest*. 2017;151(1):68–77. doi:10.1016/j.chest.2016.08.1432
11. Guo X, Sunil C, Qian G. Obesity and the development of lung fibrosis. *Front Pharmacol*. 2022;12:812166. doi:10.3389/fphar.2021.812166
12. Chen Y, Wei D, Deng M. Comparative analysis of serum proteins between hepatitis B virus genotypes B and C infection by DIA-Based quantitative proteomics. *Infect Drug Resist*. 2021;14:4701–4715. doi:10.2147/IDR.S335666
13. Moulder R, Schvartz D, Goodlett DR, Dayon L. Proteomics of diabetes, obesity, and related disorders. *Proteomics Clin Appl*. 2018;12(1):845. doi:10.1002/prca.201600134
14. López-Villar E, Martos-Moreno GÁ, Chowen JA, Okada S, Kopchick JJ, Argente J. A proteomic approach to obesity and type 2 diabetes. *J Cell Mol Med*. 2015;19(7):1455–1470. doi:10.1111/jcmm.12600
15. Hanash S. Disease proteomics. *Nature*. 2003;422(6928):226–232. doi:10.1038/nature01514
16. Herrmann C, Göke R, Richter G, Fehmann HC, Arnold R, Göke B. Glucagon-like peptide 1 and glucose-dependent insulin-releasing polypeptide plasma levels in response to nutrients. *Digestion*. 1995;56(2):117–126. doi:10.1159/000201231
17. Bullock BP, Heller RS, Habener JF. Tissue distribution of messenger ribonucleic acid encoding the rat glucagon-like peptide-1 receptor. *Endocrinology*. 1996;137(7):2968–2978. doi:10.1210/endo.137.7.8770921
18. Rayner CK, Jones KL, Horowitz M. Semaglutide vs placebo as an adjunct to intensive behavioral therapy and body weight in adults with overweight or obesity. *JAMA*. 2021;326(12):1213–1214. doi:10.1001/jama.2021.13021
19. Klonoff DC, Bassock S, Engels E, et al. Semaglutide single-dose pen-injector: post hoc analysis of summative usability testing for weight management. *Diabetes Obes Metab*. 2021;23(11):2590–2594. doi:10.1111/dom.14509

20. Fandiño J, Toba L, González-Matías LC, Diz-Chaves Y, Federico M. GLP-1 receptor agonist ameliorates experimental lung fibrosis. *Sci Rep*. 2020;10(1):18091. doi:10.1038/s41598-020-74912-1
21. Wanner C, Inzucchi SE, Lachin JM, et al. Empagliflozin and progression of kidney disease in type 2 diabetes. *N Engl J Med*. 2016;375(4):323–334. doi:10.1056/NEJMoa1515920
22. Chowdhury B, Luu AZ, Luu VZ, et al. The SGLT2 inhibitor empagliflozin reduces mortality and prevents progression in experimental pulmonary hypertension. *Biochem Biophys Res Commun*. 2020;524(1):50–56. doi:10.1016/j.bbrc.2020.01.015
23. Park HJ, Han H, Oh EY, et al. Empagliflozin and dulaglutide are effective against obesity-induced airway hyperresponsiveness and fibrosis in a murine model. *Sci Rep*. 2019;9(1):15601. doi:10.1038/s41598-019-51648-1
24. Chen X, Chen S, Li Z, et al. Effect of semaglutide and empagliflozin on cognitive function and hippocampal phosphoproteomic in obese mice. *Front Pharmacol*. 2023;17(14):975830. doi:10.3389/fphar.2023.975830
25. Chen X, Ma L, Gan K, Pan X, Chen S. Phosphorylated proteomics-based analysis of the effects of semaglutide on hippocampi of high-fat diet-induced-obese mice. *Diabetol Metab Syndr*. 2023;15(1):63. doi:10.1186/s13098-023-01023-y
26. Yue L, Chen S, Ren Q, et al. Effects of semaglutide on vascular structure and proteomics in high-fat diet-induced obese mice. *Front Endocrinol*. 2022;7(13):995007. doi:10.3389/fendo.2022.995007
27. Chen X, Ma L, Zhao J, Pan X, Chen S. Effect of empagliflozin on cytoskeletal repair in the hippocampus of obese mice. *Front Neurosci*. 2022;16:1000839. doi:10.3389/fnins.2022.1000839
28. Niu S, Ren Q, Chen S, et al. Metabolic and hepatic effects of empagliflozin on nonalcoholic fatty liver mice. *Diabetes Metab Syndr Obes*. 2023;24 (16):2549–2560. doi:10.2147/DMSO.S422327
29. Plubell DL, Wilmarth PA, Zhao Y, et al. Extended multiplexing of tandem mass tags (TMT) labeling reveals age and high fat diet specific proteome changes in mouse epididymal adipose tissue. *Mol Cell Proteomics*. 2017;16(5):873–890. doi:10.1074/mcp.M116.065524
30. Jaochico A, Sangaraju D, Shahidi-Latham SK. A rapid derivatization based lc-ms/ms method for quantitation of short chain fatty acids in human plasma and urine. *Bioanalysis*. 2019;11(8):741–753. doi:10.4155/bio-2018-0241
31. Pan X, Chen S, Chen X, et al. UTP14A, DKC1, DDX10, PinX1, and ESF1 modulate cardiac angiogenesis leading to obesity-induced cardiac injury. *J Diabetes Res*. 2022;13(2022):2923291. doi:10.1155/2022/2923291
32. O'Connell JD, Paulo JA, O'Brien JJ, Gygi SP. Proteome-wide evaluation of two common protein quantification methods. *J Proteome Res*. 2018;17 (5):1934–1942. doi:10.1021/acs.jproteome.8b00016
33. Gregg EW, Shaw JE. Global health effects of overweight and obesity. *N Engl J Med*. 2017;377(1):80–81. doi:10.1056/NEJMe1706095
34. Chang CW, Lee SM, Choi BW, et al. Costs attributable to overweight and obesity in working asthma patients in the United States. *Yonsei Med J*. 2017;58(1):187–194. doi:10.3349/ymj.2017.58.1.187
35. André DM, Calixto MC, Sollon C, et al. High-fat diet-induced obesity impairs insulin signaling in lungs of allergen-challenged mice: improvement by resveratrol. *Sci Rep*. 2017;7(1):17296. doi:10.1038/s41598-017-17558-w
36. Singh S, Bodas M, Bhatraju NK, et al. Hyperinsulinemia adversely affects lung structure and function. *Am J Physiol Lung Cell Mol Physiol*. 2016;310(9):L837–45. doi:10.1152/ajplung.00091.2015
37. Richter G, Feddersen O, Wagner U, Barth P, Göke R, Göke B. GLP-1 stimulates secretion of macromolecules from airways and relaxes pulmonary artery. *Am J Physiol*. 1993;265(4 Pt 1):L374–81. doi:10.1152/ajplung.1993.265.4.L374
38. Benito E, Blazquez E, Bosch MA. Glucagon-like peptide-1-(7-36)amide increases pulmonary surfactant secretion through a cyclic adenosine 3′,5′-monophosphate-dependent protein kinase mechanism in rat type II pneumocytes. *Endocrinology*. 1998;139(5):2363–2368. doi:10.1210/endo.139.5.5998
39. Vara E, Arias-Díaz J, Garcia C, Balibrea JL, Blázquez E. Glucagon-like peptide-1(7-36) amide stimulates surfactant secretion in human type II pneumocytes. *Am J Respir Crit Care Med*. 2001;163(4):840–846. doi:10.1164/ajrccm.163.4.9912132
40. Romaní-Pérez M, Outeiriño-Iglesias V, Moya CM, et al. Activation of the GLP-1 receptor by liraglutide increases ACE2 expression, reversing right ventricle hypertrophy, and improving the production of SP-A and SP-B in the lungs of type 1 diabetes rats. *Endocrinology*. 2015;156 (10):3559–3569. doi:10.1210/en.2014-1685
41. Jiang Z, Tan J, Yuan Y, Shen J, Chen Y. Semaglutide ameliorates lipopolysaccharide-induced acute lung injury through inhibiting HDAC5-mediated activation of NF-κB signaling pathway. *Hum Exp Toxicol*. 2022;41:9603271221125931. doi:10.1177/09603271221125931
42. Yang X, Feng P, Zhang X, et al. The diabetes drug semaglutide reduces infarct size, inflammation, and apoptosis, and normalizes neurogenesis in a rat model of stroke. *Neuropharmacology*. 2019;158:107748. doi:10.1016/j.neuropharm.2019.107748
43. El-Horany HE, Atef MM, Ghafar MTA, et al. Empagliflozin ameliorates bleomycin-induced pulmonary fibrosis in rats by modulating Sesn2/AMPK/Nrf2 signaling and targeting ferroptosis and autophagy. *Int J Mol Sci*. 2023;24(11):9481. doi:10.3390/ijms24119481
44. Gokbulut P, Kuskonmaz SM, Koc G, et al. Evaluation of the effects of empagliflozin on acute lung injury in rat intestinal ischemia-reperfusion model. *J Endocrinol Invest*. 2023;46(5):1017–1026. doi:10.1007/s40618-022-01978-1
45. Huang D, Ju F, Du L, et al. Empagliflozin protects against pulmonary ischemia/reperfusion injury via an extracellular signal-regulated kinases 1 and 2-dependent mechanism. *J Pharmacol Exp Ther*. 2022;380(3):230–241. doi:10.1124/jpet.121.000956
46. Castoldi G, Carletti R, Ippolito S, et al. Renal anti-fibrotic effect of sodium glucose cotransporter 2 inhibition in angiotensin II-dependent hypertension. *Am J Nephrol*. 2020;51(2):119–129. doi:10.1159/000505144
47. Heo YJ, Lee N, Choi SE, et al. Empagliflozin reduces the progression of hepatic fibrosis in a mouse model and inhibits the activation of hepatic stellate cells via the hippo signalling pathway. *Biomedicines*. 2022;10(5):1032. doi:10.3390/biomedicines10051032
48. Kabel AM, Estfanous RS, Alrobaian MM. Targeting oxidative stress, proinflammatory cytokines, apoptosis and toll like receptor 4 by empagliflozin to ameliorate bleomycin-induced lung fibrosis. *Respir Physiol Neurobiol*. 2020;273:103316. doi:10.1016/j.resp.2019.103316
49. Pan X, Chen S, Chen X, et al. Effect of high-fat diet and empagliflozin on cardiac proteins in mice. *Nutr Metab*. 2022;19(1):69. doi:10.1186/s12986-022-00705-0
50. Ge XN, Greenberg Y, Hosseinkhani MR, et al. High-fat diet promotes lung fibrosis and attenuates airway eosinophilia after exposure to cockroach allergen in mice. *Exp Lung Res*. 2013;39(9):365–378. doi:10.3109/01902148.2013.829537
51. Li ZG, Xie WB, Escano CS, et al. Response gene to complement 32 is essential for fibroblast activation in renal fibrosis. *J Biol Chem*. 2011;286 (48):41323–41330. doi:10.1074/jbc.M111.259184

52. Luzina IG, Rus V, Lockatell V, et al. Regulator of cell cycle protein (RGCC/RGC-32) protects against pulmonary fibrosis. *Am J Respir Cell Mol Biol*. 2022;66(2):146–157. doi:10.1165/rcmb.2021-0022OC
53. Stapor PC, Azimi MS, Ahsan T, Murfee WL. An angiogenesis model for investigating multicellular interactions across intact microvascular networks. *Am J Physiol Heart Circ Physiol*. 2013;304(2):H235–45. doi:10.1152/ajpheart.00552.2012
54. Banerji S, Ni J, Wang SX, et al. LYVE-1, a new homologue of the CD44 glycoprotein, is a lymph-specific receptor for hyaluronan. *J Cell Biol*. 1999;144(4):789–801. doi:10.1083/jcb.144.4.789
55. Jackson DG. Biology of the lymphatic marker LYVE-1 and applications in research into lymphatic trafficking and lymphangiogenesis. *APMIS*. 2004;112(7–8):526–538. doi:10.1111/j.1600-0463.2004.apm11207-0811.x
56. Akishima Y, Ito K, Zhang L, et al. Immunohistochemical detection of human small lymphatic vessels under normal and pathological conditions using the LYVE-1 antibody. *Virchows Arch*. 2004;444(2):153–157. doi:10.1007/s00428-003-0950-8
57. Alexander JS, Chaitanya GV, Grisham MB, Boktor M. Emerging roles of lymphatics in inflammatory bowel disease. *Ann N Y Acad Sci*. 2010;1207 (Suppl 1):E75–E85. doi:10.1111/j.1749-6632.2010.05757.x.
58. Alitalo K. The lymphatic vasculature in disease. *Nat Med*. 2011;17(11):1371–1380. doi:10.1038/nm.2545
59. Cui Y, Liu K, Lamattina AM, Visner G, El-Chemaly S. Lymphatic vessels: the next frontier in lung transplant. *Ann Am Thorac Soc*. 2017;14 (Supplement_3):S226–S232. doi:10.1513/AnnalsATS.201606-465MG
60. Stump B, Cui Y, Kidambi P, Lamattina AM, El-Chemaly S. Lymphatic changes in respiratory diseases: more than just remodeling of the lung? Am. *J Respir Cell Mol Biol*. 2017;57(3):272–279. doi:10.1165/rcmb.2016-0290TR
61. Wang L, Chen Q, Liu TT, et al. Role and mechanism of benzo[a]pyrene in the transformation of chronic obstructive pulmonary disease into lung adenocarcinoma. *J Cancer Res Clin Oncol*. 2023;149(8):4741–4760. doi:10.1007/s00432-022-04353-y
62. Nunomiya K, Shibata Y, Abe S, et al. Relationship between serum level of lymphatic vessel endothelial hyaluronan receptor-1 and prognosis in patients with lung cancer. *J Cancer*. 2014;5(3):242–247. doi:10.7150/jca.8486
63. Johnson LA, Prevo R, Clasper S, Jackson DG. Inflammation-induced uptake and degradation of the lymphatic endothelial hyaluronan receptor LYVE-1. *JBio Chem*. 2007;282(46):33671–33680. doi:10.1074/jbc.M702889200
64. Fang JY, Richardson BC. The MAPK signalling pathways and colorectal cancer. *Lancet Oncol*. 2005;6(5):322–327. doi:10.1016/S1470-2045(05) 70168-6
65. Hashimoto S, Gon Y, Takeshita I, Matsumoto K, Maruoka S, Horie T. Transforming growth Factor-beta1 induces phenotypic modulation of human lung fibroblasts to myofibroblast through a c-Jun-NH2-terminal kinase-dependent pathway. *Am J Respir Crit Care Med*. 2001;163(1):152–157. doi:10.1164/ajrccm.163.1.2005069
66. Guo H, Jian Z, Liu H, et al. TGF-β1-induced EMT activation via both Smad-dependent and MAPK signaling pathways in Cu-induced pulmonary fibrosis. *Toxicol Appl Pharmacol*. 2021;1(418):115500. doi:10.1016/j.taap.2021.115500
67. Boucherat O, Landry-Truchon K, Aoidi R, et al. Lung development requires an active ERK/MAPK pathway in the lung mesenchyme. *Dev Dyn*. 2017;246(1):72–82. doi:10.1002/dvdy.24464
68. Pearson G, Robinson F, Beers Gibson T, et al. Mitogen-activated protein (MAP) kinase pathways: regulation and physiological functions. *Endocr Rev*. 2001;22(2):153–183. doi:10.1210/edrv.22.2.0428
69. Sun Y, Liu WZ, Liu T, Feng X, Yang N, Zhou HF. Signaling pathway of MAPK/ERK in cell proliferation, differentiation, migration, senescence and apoptosis. *J Recept Signal Transduction Res*. 2015;35(6):600–604. doi:10.3109/10799893.2015.1030412
70. Kranz A, Kinner A, Kolling R, Pelham HRB. A family of small coiled-coil-forming proteins functioning at the late endosome in yeast. *Mol Biol Cell*. 2001;12(3):711–723. doi:10.1091/mbc.12.3.711
71. Shim JH, Xiao C, Hayden MS, et al. CHMP5 is essential for late endosome function and down-regulation of receptor signaling during mouse embryogenesis. *J Cell Biol*. 2006;172(7):1045–1056. doi:10.1083/jcb.200509041
72. Shahmoradgoli M, Mannherz O, Engel F, et al. Antiapoptotic function of charged multivesicular body protein 5: a potentially relevant gene in acute myeloid leukemia. *Int, J, Cancer*. 2011;128(12):2865–2871. doi:10.1002/ijc.25632
73. Nakova VV, Nakov Z, Dokuzova S, Prosheva T, Krstevska B. Efficacy and safety of empagliflozin and semaglutide (Once Weekly) in T2DM patients in shtip. *Pril*. 2023;44(1):71–77. doi:10.2478/prilozi-2023-0008
74. Sivalingam S, Wasehuus VS, Curovic VR, et al. Albuminuria-lowering effect of adding semaglutide on top of empagliflozin in individuals with type 2 diabetes: a randomized and placebo-controlled study. *Diabetes Obes Metab*. 2024;26(1):54–64. doi:10.1111/dom.15287
75. Davies MJ, Aroda VR, Collins BS, et al. Management of hyperglycemia in type 2 Diabetes, 2022. A consensus report by the American diabetes Association (ADA) and the European Association for the Study of Diabetes (EASD). *Diabetes Care*. 2022;45(11):2753–2786. doi:10.2337/dci22-0034
76. Vernstrøm L, Gullaksen S, Sørensen SS, Funck KL, Laugesen E, Poulsen PL. Separate and combined effects of empagliflozin and semaglutide on vascular function: a 32-week randomized trial. *Diabetes Obes Metab*. 2024;19:doi:10.1111/dom.15464